



Shahid Chamran
University of Ahvaz

Journal of Applied and Computational Mechanics



Research Paper

Application of a Generalized Isotropic Yield Criterion to Determining Limit Load Solutions for Highly Undermatched Welded Bars in Tension

Sergei Alexandrov^{1,2,3}, Stanislav Strashnov⁴, Yong Li²

¹ Ishlinsky Institute for Problems in Mechanics RAS, 101-1 Prospect Vernadskogo, Moscow, 119526, Russian Federation, Email: sergei_alexandrov@spartak.ru

² School of Mechanical Engineering and Automation, Beihang University, No. 37 Xueyuan Road, Beijing, 100191, China, Email: sergei_alexandrov@spartak.ru (S.A.); liyong19@buaa.edu.cn (Y.L.)

³ Department of Civil Engineering, RUDN University, 6 Miklukho-Maklaya St, Moscow, 117198, Russian Federation, Email: alexandrov-se@rudn.ru

⁴ Department of Applied Informatics and Intelligent Systems in Humanities, RUDN University, 6 Miklukho-Maklaya St, Moscow, 117198, Russian Federation, Email: shtrafnoy@gmail.com

Received October 03 2023; Revised January 17 2024; Accepted for publication February 03 2024.

Corresponding author: Y. Li (liyong19@buaa.edu.cn)

© 2024 Published by Shahid Chamran University of Ahvaz

Abstract. The limit load is an important input parameter of analytical flaw assessment procedures. The accuracy of limit load solutions affects the accuracy of these procedures. The present paper evaluates the influence of a class of the work functions involved in the upper bound theorem on the upper bound limit load of a round highly undermatched tensile bar. It is assumed that the weld contains a crack. The boundary value problem is axisymmetric. The work functions considered cover the entire range of physically reasonable yield criteria, assuming the material is isotropic and incompressible. The kinematically admissible velocity field chosen accounts for some features of the real velocity field. In particular, the kinematically admissible velocity field is singular near the interface between the base material and weld. As a result, the new solution predicts a more accurate limit load than available solutions for the von Mises and Tresca yield criteria. Moreover, the effect of the generalized yield criterion associated with the work functions above on the limit load is shown.

Keywords: Limit load; upper bound theorem; highly undermatched structure; generalized yield criterion.

1. Introduction

The importance of analytical models in fatigue and fracture mechanics has been emphasized in [1]. In particular, analytical flaw assessment procedures are widely used in engineering practice for the assessment of the remaining load capacity of structures containing a crack [2]. An important class of such structures is welded structures containing cracks and other defects in the weld. The welded structures are conveniently divided into two groups. One of these groups includes overmatched structures (i.e., the base material is softer than the weld) and the other undermatched structures (i.e., the weld is softer than the base material). However, sometimes a portion of the weld is softer than the base material, and the remainder is stronger [3]. Undermatched welded joints are important for several industry sectors. Several examples of using such joints have been reported in [4–7]. Limit load solutions are required to apply flaw assessment procedures to undermatched welded joints. In some cases, the difference between the yield stresses of the weld and base material is so high that the weld becomes fully plastic under loading, whereas the base material is elastic [8, 9]. Such welded joints are named highly undermatched welded joints.

The limit load is an essential input parameter of the analytical flaw assessment procedures [2]. Many limit load solutions for highly undermatched welded joints are available in the literature. A review of such solutions has been presented in [8]. Most of these solutions are under plane strain conditions. A distinguished feature of plane strain solutions is the independence of the dimensionless limit load on the yield criterion. The reason for this feature is two-fold. Firstly, the limit load is independent of the elastic properties of materials [10]. Secondly, any plane strain pressure-independent yield criterion for isotropic perfectly plastic materials postulates that the difference between the two principal stresses in a generic flow plane is constant [11, 12]. However, in the case of other deformation modes, the yield criterion can affect the limit load. It is worthy of note that the effect of anisotropic yield criteria on the limit load has been intensively investigated in the literature. Several limit load solutions for anisotropic yield criteria have been provided in [13–15]. In particular, it has been shown that this effect can be significant. Therefore, investigating the effect of various isotropic yield criteria on the limit load is important. A study on the fracture behavior of welded joints with multiple defects has been presented in [16]. The present paper aims to show the effect of generalized isotropic yield criteria on the



limit load of an axisymmetric highly undermatched welded rod subject to tension. It is assumed that a circular crack is located in the weld.

Two upper bound solutions for the specimen above have been proposed in [17]. One of these solutions is for the von Mises yield criterion, and the other for Tresca's. In either case, standard formulations of the upper bound theorem presented in textbooks apply. Using a generalized yield criterion requires the formulation given in [18]. To the best of the authors' knowledge, this formulation has never been applied in fracture mechanics. One difficulty is that the theorem proven in [18] involves the work function. An explicit function representing the yield criterion associated with a given work function cannot readily be expressed except for some particular cases, such as the von Mises and Tresca yield criteria. However, the two work functions introduced in [19] can closely approximate any isotropic pressure-independent yield criterion. In particular, one of them closely represents a widely used generalized yield criterion proposed in [20]. The two work functions above are adopted in the present paper.

In the case of highly undermatched welded joints, the bi-material interface is usually a velocity discontinuity surface. An important mathematical feature of such surfaces is that the real velocity field in the plastic material is singular [21]. In particular, some strain rate components approach infinity or negative infinity. This feature has been successfully used for constructing kinematically admissible velocity fields in conjunction with the von Mises and Tresca yield criteria [17, 22]. However, the theoretical result in [21] applies to any isotropic yield criterion. The present paper combines this result with the work functions [19] for deriving a new upper bound limit load.

The general procedure for calculating the limit load is illustrated with a numerical example. This example shows the effect of the isotropic yield criterion on the limit load of a highly undermatched welded rod with a crack subject to uniaxial tension. This general solution provides a solution for the von Mises criterion at a specific value of parameters involved in the work functions. Another solution for this yield criterion has been provided in [23], where compression of a solid disk has been considered. A comparison of the two solutions shows that the new solution predicts a better estimate of the limit load for this particular case. It is worthy of note that the difference between tension and compression is immaterial for pressure-independent materials if the tensile specimen contains no crack. It is because any kinematically admissible velocity field for the tensile specimen can be obtained from a kinematically admissible velocity field for the compressed specimen by changing the sense of the velocity components.

2. Statement of the Problem

A round welded bar is subject to tension. The bar's radius is R_0 , and the half-thickness of the weld is H . A circular crack is located at the middle plane of the weld. Its radius is a_0 . The tensile force is denoted as F . It is supposed that the weld is much softer than the base material such that plastic deformation localizes in the weld. The base material is elastic. It may be regarded as rigid for limit analysis [10]. The velocity of each block of rigid material is V . Its magnitude is immaterial for rate-independent models. A schematic diagram of the bar is depicted in Fig. 1.

The overall objective of this research is to evaluate the tensile force at plastic collapse.

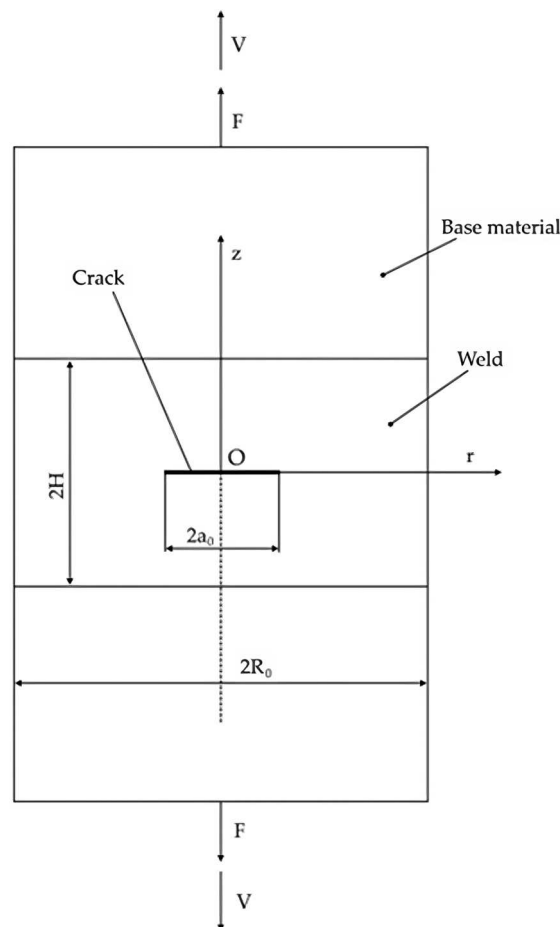


Fig. 1. Schematic diagram of the specimen.



It is assumed that the weld obeys a generalized isotropic yield criterion. It is known that the Tresca and Schmidt–Ishlinskii yield criteria form two extreme bounds for all physically reasonable pressure-independent isotropic yield criteria [20]. However, the upper bound theorem presented in [18] requires the work function rather than the yield criterion. In general, the work function associated with a given yield criterion cannot be represented by an explicit function. However, it is possible to formulate two work functions such that the associated yield criteria cover the entire domain between the two extreme bounds above [19]. Let σ_0 be the yield stress in tension. One of these work functions is:

$$E = E_1 = \sigma_0 \frac{2^{(t-1)/t}}{3} \sqrt[t]{(\xi_1 - \xi_2)^t + (\xi_2 - \xi_3)^t + (\xi_1 - \xi_3)^t} \quad (1)$$

and the other is

$$E = E_2 = \begin{cases} \sigma_0 \frac{2}{3} (2 + 2^m)^{-1/m} \sqrt[m]{(2\xi_1 - \xi_2 - \xi_3)^m + (2\xi_2 - \xi_1 - \xi_3)^m + (-2\xi_3 + \xi_2 + \xi_1)^m} & \text{for } 2\xi_2 - \xi_1 - \xi_3 \geq 0 \\ \sigma_0 \frac{2}{3} (2 + 2^m)^{-1/m} \sqrt[m]{(2\xi_1 - \xi_2 - \xi_3)^m + (-2\xi_2 + \xi_1 + \xi_3)^m + (-2\xi_3 + \xi_2 + \xi_1)^m} & \text{for } 2\xi_2 - \xi_1 - \xi_3 \leq 0 \end{cases} \quad (2)$$

Here ξ_1 , ξ_2 and ξ_3 are the principal strain rates satisfying the inequalities:

$$\xi_1 \geq \xi_2 \geq \xi_3. \quad (3)$$

Also, t and m are constitutive parameters. It is possible to check by inspection that the work function E_1 is associated with the von Mises yield criterion at $t = 2$ and the Schmidt–Ishlinskii yield criterion as $t \rightarrow \infty$. Similarly, the work function E_2 is associated with the von Mises yield criterion at $m = 2$ and the Tresca yield criterion as $m \rightarrow \infty$. Thus, the work functions allow one to cover the entire domain between the Tresca and Schmidt–Ishlinskii yield criteria as $2 \leq t < \infty$ and $2 \leq m < \infty$.

The solution in the next sections is in the cylindrical coordinate system (r, θ, z) shown in Fig. 1. It is convenient to use the following dimensionless quantities:

$$\rho = \frac{r}{R_0}, \quad \zeta = \frac{z}{H}, \quad h = \frac{H}{R_0}, \quad \text{and} \quad a = \frac{a_0}{R_0}. \quad (4)$$

3. Kinematically Admissible Velocity Field

Because of symmetry, the half-space $z \geq 0$ needs to be considered. The general structure of the kinematically admissible velocity field is shown in Fig. 2. The region on the left to line AB is rigid. This region moves along with the rigid base material with velocity V . The region on the right to line AB is plastic. AB and BC are velocity discontinuity lines.

Let u_r and u_z be the radial and axial velocities in the cylindrical coordinate system. The velocity boundary conditions are $u_z = 0$ for $z = 0$ and $u_z = V$ for $z = H$. Then, using (4), it is reasonable to assume that:

$$u_z = V\zeta \quad (5)$$

in the plastic region. In particular, this assumption applies in Prandtl's solution for the plane strain compression of a plastic layer between two plates (see, for example, [11]). An accurate numerical solution [12] has confirmed the high accuracy of this approximate solution.

In the cylindrical coordinate system, the equation of incompressibility is represented as

$$\frac{\partial u_r}{\partial r} + \frac{u_r}{r} + \frac{\partial u_z}{\partial z} = 0. \quad (6)$$

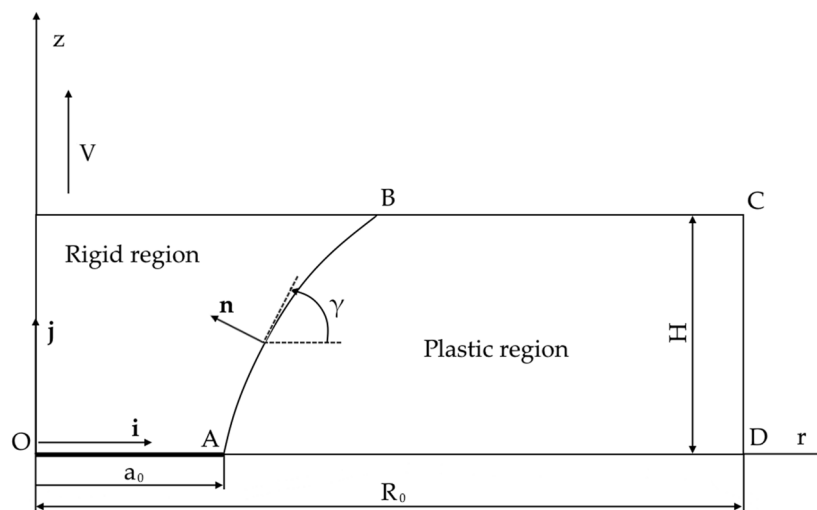


Fig. 2. General structure of the kinematically admissible velocity field.



Using equations (4) and (5), one can transform Eq. (6) to:

$$\frac{\partial(\rho u_r)}{\partial \rho} = -\frac{V}{h} \rho. \quad (7)$$

This equation can be immediately integrated to give:

$$\frac{u_r}{V} = \frac{g(\zeta)}{\rho} - \frac{\rho}{2h}. \quad (8)$$

Here $g(\zeta)$ is an arbitrary function of ζ . Using equations (5) and (8), one can represent the velocity vector in the plastic region as:

$$\mathbf{u}^{(p)} = V \left(\frac{g(\zeta)}{\rho} - \frac{\rho}{2h} \right) \mathbf{i} + V\zeta \mathbf{j}, \quad (9)$$

where \mathbf{i} and \mathbf{j} are the unit base vectors of the cylindrical coordinate system directed along the r - and z - axes, respectively. The rigid region moves along the z -axis (Fig. 2). Therefore, its velocity is:

$$\mathbf{u}^{(r)} = V\mathbf{j}. \quad (10)$$

For further convenience, equation (9) is rewritten as:

$$\mathbf{u}^{(p)} = Vf(\beta, \zeta) \mathbf{i} + V\zeta \mathbf{j}, \quad (11)$$

where

$$\beta = \rho^2 \quad \text{and} \quad f(\beta, \zeta) = \left(g(\zeta) - \frac{\beta}{2h} \right) \frac{1}{\sqrt{\beta}}. \quad (12)$$

The velocity is discontinuous along line AB (Fig. 2). However, the normal velocity must be continuous across this line. Let \mathbf{n} be the normal vector to line AB . It follows from the geometry of Fig. 2 that:

$$\mathbf{n} = -\mathbf{i} \sin \gamma + \mathbf{j} \cos \gamma. \quad (13)$$

Here γ is the angle between the radial coordinate and the tangent to line AB measured from the coordinate anticlockwise. The condition that the normal velocity is continuous can be represented as $\mathbf{n} \cdot \mathbf{u}^{(r)} = \mathbf{n} \cdot \mathbf{u}^{(p)}$. It is understood here that $\mathbf{u}^{(r)}$ and $\mathbf{u}^{(p)}$ are calculated at line AB . Substituting equations (10), (11), and (13) into this equation yields:

$$\tan \gamma = -\frac{(1-\zeta)}{f(\beta, \zeta)}. \quad (14)$$

Using trigonometric identities, one can get from this equation:

$$\sin \gamma = \frac{(1-\zeta)}{\sqrt{f^2 + (1-\zeta)^2}} \quad \text{and} \quad \cos \gamma = -\frac{f}{\sqrt{f^2 + (1-\zeta)^2}}. \quad (15)$$

It has been taken into account here that $0 < \gamma < \pi$. It follows from the geometry of Fig. 2, Eqs. (4) and (12) that:

$$\tan \gamma = \frac{dz}{dr} = \frac{H d\zeta}{R_0 d\rho} = h \frac{d\zeta}{d\rho} = 2h\sqrt{\beta} \frac{d\zeta}{d\beta}. \quad (16)$$

Equations (14) and (16) combine to give:

$$\frac{d\beta}{d\zeta} = -2h\sqrt{\beta} \frac{f(\beta, \zeta)}{(1-\zeta)}. \quad (17)$$

Eliminating $f(\beta, \zeta)$ here using the second equation in (12) results in the following linear differential equation for β :

$$\frac{d\beta}{d\zeta} = \frac{\beta - 2hg(\zeta)}{(1-\zeta)}. \quad (18)$$

Its general solution is:

$$\beta = \beta_d(\zeta) = \left[C - 2h \int_1^\zeta g(\omega) d\omega \right] \frac{1}{(1-\zeta)}. \quad (19)$$

Here C is constant. It is seen from this solution that β is finite at $\zeta = 1$ only if $C = 0$. Putting $C = 0$, one transforms Eq. (19) to:

$$\beta = \beta_d(\zeta) = \frac{2h}{(1-\zeta)} \int_\zeta^1 g(\omega) d\omega. \quad (20)$$



The right-hand side of this equation reduces to the expression $0/0$ as $\zeta \rightarrow 1$. Applying l'Hospital's rule gives:

$$\beta_B = 2hg(1). \quad (21)$$

Here β_B is the value of β at point B (Fig. 2). The first equation in (12) and equation (20) determine the shape of the velocity discontinuity line. Therefore, constructing the kinematically admissible velocity field has been completed.

4. Limit Load

The plastic work rate below is calculated assuming the plastic region is in contact with the base material over a finite domain. Using Eq. (21), one can express this condition as:

$$2hg(1) < 1. \quad (22)$$

This inequality will be verified a posteriori. It is necessary to calculate the plastic work rate in the volume, W_V , at the velocity discontinuity surface AB, W_{AB} , and at the velocity discontinuity surface BC, W_{BC} .

The plastic work rate in the volume is:

$$W_V = 2\pi \int_0^H \int_{r_{AB}(z)}^{R_0} E r dr dz. \quad (23)$$

Here $r = r_{AB}(z)$ is the equation of the velocity discontinuity line AB. Using equation (4) and the first equation in (12), one can transform equation (23) to:

$$W_V = \pi H R_0^2 \int_0^1 \int_{\beta_d(\zeta)}^1 E d\beta d\zeta. \quad (24)$$

It is seen from equations (1) and (2) that it is necessary to calculate the principal strain rates to determine the integrand. The non-zero strain rate components in the cylindrical coordinate system are expressed through the radial and axial velocities as:

$$\xi_{rr} = \frac{\partial u_r}{\partial r}, \quad \xi_{\theta\theta} = \frac{u_r}{r}, \quad \xi_{zz} = \frac{\partial u_z}{\partial z}, \quad \text{and} \quad \xi_{rz} = \frac{1}{2} \left(\frac{\partial u_z}{\partial r} + \frac{\partial u_r}{\partial z} \right). \quad (25)$$

Substituting equations (5) and (8) into equation (25) and using equations (4) and (12) leads to:

$$\xi_{rr} = -\frac{V}{R_0} \left(\frac{1}{2h} + \frac{g(\zeta)}{\beta} \right), \quad \xi_{\theta\theta} = \frac{V}{R_0} \left(\frac{g(\zeta)}{\beta} - \frac{1}{2h} \right), \quad \xi_{zz} = \frac{V}{H}, \quad \text{and} \quad \xi_{rz} = \frac{V}{2H\sqrt{\beta}} \frac{dg}{d\zeta}. \quad (26)$$

It is convenient to rewrite these expressions as:

$$\xi_{rr} = \frac{V}{H} \varepsilon_{rr}, \quad \xi_{\theta\theta} = \frac{V}{H} \varepsilon_{\theta\theta}, \quad \xi_{zz} = \frac{V}{H}, \quad \text{and} \quad \xi_{rz} = \frac{V}{H} \varepsilon_{rz}, \quad (27)$$

where

$$\varepsilon_{rr} = -\frac{1}{2} - \frac{hg(\zeta)}{\beta}, \quad \varepsilon_{\theta\theta} = \frac{hg(\zeta)}{\beta} - \frac{1}{2}, \quad \text{and} \quad \varepsilon_{rz} = \frac{1}{2\sqrt{\beta}} \frac{dg}{d\zeta}. \quad (28)$$

The circumferential strain rate is one of the principal strain rates, $\xi_{\theta\theta} = \xi_2$. The other principal strain rates are determined as:

$$\xi_1 = \frac{\xi_{rr} + \xi_{zz}}{2} + \frac{1}{2} \sqrt{(\xi_{rr} - \xi_{zz})^2 + 4\xi_{rz}^2} \quad \text{and} \quad \xi_3 = \frac{\xi_{rr} + \xi_{zz}}{2} - \frac{1}{2} \sqrt{(\xi_{rr} - \xi_{zz})^2 + 4\xi_{rz}^2}. \quad (29)$$

Using equations (27) and (28), one can transform equation (29) to:

$$\xi_1 = \frac{V}{H} \varepsilon_1 \quad \text{and} \quad \xi_3 = \frac{V}{H} \varepsilon_3, \quad (30)$$

where

$$\varepsilon_1 = \frac{1}{2} \left(\frac{1}{2} - \frac{hg(\zeta)}{\beta} \right) + \frac{1}{2} \sqrt{\left(\frac{3}{2} + \frac{hg(\zeta)}{\beta} \right) + \frac{1}{\beta} \left(\frac{dg}{d\zeta} \right)^2}, \quad (31)$$

$$\varepsilon_3 = \frac{1}{2} \left(\frac{1}{2} - \frac{hg(\zeta)}{\beta} \right) - \frac{1}{2} \sqrt{\left(\frac{3}{2} + \frac{hg(\zeta)}{\beta} \right) + \frac{1}{\beta} \left(\frac{dg}{d\zeta} \right)^2}.$$

Equations (1) and (2) can be rewritten as:

$$E_1 = \frac{\sigma_0 V}{H} e_1 \quad \text{and} \quad E_2 = \frac{\sigma_0 V}{H} e_2, \quad (32)$$

where



$$e_1 = \frac{2^{(t-1)/t}}{3} \sqrt[t]{(\varepsilon_1 - \varepsilon_2)^t + (\varepsilon_2 - \varepsilon_3)^t + (\varepsilon_1 - \varepsilon_3)^t},$$

$$e_2 = \begin{cases} \frac{2}{3} (2 + 2^m)^{-1/m} \sqrt[m]{(2\varepsilon_1 - \varepsilon_2 - \varepsilon_3)^m + (2\varepsilon_2 - \varepsilon_1 - \varepsilon_3)^m + (-2\varepsilon_3 + \varepsilon_2 + \varepsilon_1)^m} & \text{for } 2\varepsilon_2 - \varepsilon_1 - \varepsilon_3 \geq 0 \\ \frac{2}{3} (2 + 2^m)^{-1/m} \sqrt[m]{(2\varepsilon_1 - \varepsilon_2 - \varepsilon_3)^m + (-2\varepsilon_2 + \varepsilon_1 + \varepsilon_3)^m + (-2\varepsilon_3 + \varepsilon_2 + \varepsilon_1)^m} & \text{for } 2\varepsilon_2 - \varepsilon_1 - \varepsilon_3 \leq 0 \end{cases}. \quad (33)$$

Here $\varepsilon_2 = \xi_2 H/V$. Substituting equation (32) into equation (24) gives:

$$\frac{W_V}{\pi V R_0^2 \sigma_0} = \int_0^1 \int_{\beta_d(\zeta)}^1 e_1 d\beta d\zeta \quad \text{and} \quad \frac{W_V}{\pi V R_0^2 \sigma_0} = \int_0^1 \int_{\beta_d(\zeta)}^1 e_2 d\beta d\zeta \quad (34)$$

for $E = E_1$ and $E = E_2$, respectively. The right-hand sides of these equations can be evaluated numerically for any given function $g(\zeta)$. The plastic work rate at the velocity discontinuity surface AB is:

$$W_{AB} = 2\pi k \int_{AB} r [u] dS. \quad (35)$$

Here k is the shear yield stress and $[u]$ is the amount of velocity jump. The latter is determined as:

$$[u] = |\mathbf{u}^{(r)} - \mathbf{u}^{(p)}|. \quad (36)$$

It follows from equations (10), (11), and (36) that:

$$[u] = V \sqrt{(1 - \zeta)^2 + f^2}. \quad (37)$$

Utilizing equation (15), one can rewrite this equation as:

$$[u] = V \frac{(1 - \zeta)}{\sin \gamma}. \quad (38)$$

By definition,

$$dS = \sqrt{(dr)^2 + (dz)^2} = \sqrt{\left(\frac{dr}{dz}\right)^2 + 1} dz. \quad (39)$$

Utilizing the first equation in (16) and equation (4), one can transform equation (39) to:

$$dS = \frac{H d\zeta}{\sin \gamma}. \quad (40)$$

Eliminating dS and $[u]$ in equation (35) using equations (38) and (40) leads to:

$$\frac{W_{AB}}{\pi V R_0^2 \sigma_0} = 2 \left(\frac{k}{\sigma_0} \right) h \int_0^1 \sqrt{\beta_d(\zeta)} \frac{(1 - \zeta)}{\sin^2 \gamma} d\zeta. \quad (41)$$

Using equations (16), (18), and (19), one can evaluate the right-hand side of this equation numerically for any given function $g(\zeta)$. The plastic work rate at the velocity discontinuity surface BC is:

$$W_{BC} = 2\pi k \int_{r_B}^{R_0} r |u_r| dr. \quad (42)$$

It is understood here that the radial velocity is calculated at $\zeta = 1$. Using equations (4), (8) and (21), one can transform equation (42) to:

$$W_{BC} = \frac{\pi V R_0^2 k}{h} \int_{\beta_B}^1 (\rho^2 - \beta_B) d\rho. \quad (43)$$

Integrating results in:

$$\frac{W_{BC}}{\pi V R_0^2 \sigma_0} = \frac{1}{h} \left(\frac{k}{\sigma_0} \right) \left[\frac{1}{3} - \beta_B + \frac{2}{3} \beta_B \sqrt{\beta_B} \right]. \quad (44)$$

The shear yield stress involved in equations (41) and (44) depends on the work function and is given by [19]:

$$\frac{k}{\sigma_0} = \frac{(1 + 2^{t-1})^{1/t}}{3} \quad \text{and} \quad \frac{k}{\sigma_0} = (1 + 2^{m-1})^{-1/m} \quad (45)$$

for $E = E_1$ and $E = E_2$, respectively.



According to the theorem [18], an upper bound on the limit load is estimated as $F_u V = W_V + W_{AB} + W_{BC}$. Then, the dimensionless upper bound limit load is:

$$f_u = \frac{F_u}{\pi R_0^2 \sigma_0} = \frac{W_V}{\pi V R_0^2 \sigma_0} + \frac{W_{AB}}{\pi V R_0^2 \sigma_0} + \frac{W_{BC}}{\pi V R_0^2 \sigma_0}. \quad (46)$$

Equations (34), (41), and (44) allow for the right-hand side of this equation to be calculated for any given function $g(\zeta)$.

5. Numerical Example

5.1. Function $g(\zeta)$

Symmetry dictates that $g(\zeta)$ is an even function of ζ . Moreover, the general theory [16] requires that $dg/d\zeta = O(1/\sqrt{1-\zeta})$ as $\zeta \rightarrow 1$. One of the simplest functions satisfying both conditions is:

$$g(\zeta) = g_0 \sqrt{1-\zeta^2} + g_1, \quad (47)$$

where g_0 and g_1 are constant. Substituting equation (47) into equation (20) and integrating yields:

$$\beta_d(\zeta) = 2hg_1 + \frac{hg_0}{(1-\zeta)} \left(\frac{\pi}{2} - \zeta \sqrt{1-\zeta^2} - \arcsin \zeta \right). \quad (48)$$

This velocity discontinuity line should pass through the crack tip for the velocity field to be kinematically admissible. Therefore, taking into account the definition for β , $\beta_d(0) = a^2$. Using this condition, one can get from equation (48):

$$g_0 = \frac{2(a^2 - 2hg_1)}{\pi h}. \quad (49)$$

Moreover, it follows from equations (21) and (47) that $\beta_b = 2hg_1$. Employing this equation and equation (49), one can transform equations (47) and (48) to:

$$g(\zeta) = \frac{2(a^2 - \beta_b) \sqrt{1-\zeta^2}}{\pi h} + \frac{\beta_b}{2h} \quad (50)$$

and

$$\beta_d(\zeta) = \beta_b + \frac{2(a^2 - \beta_b)}{\pi(1-\zeta)} \left(\frac{\pi}{2} - \zeta \sqrt{1-\zeta^2} - \arcsin \zeta \right) \quad (51)$$

respectively.

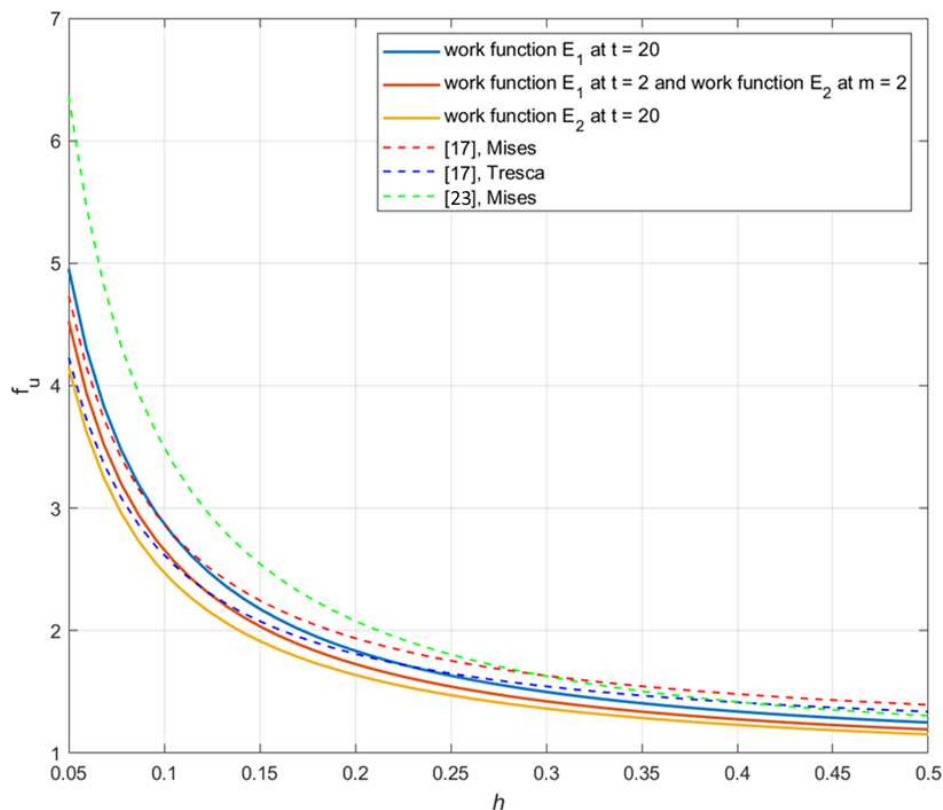
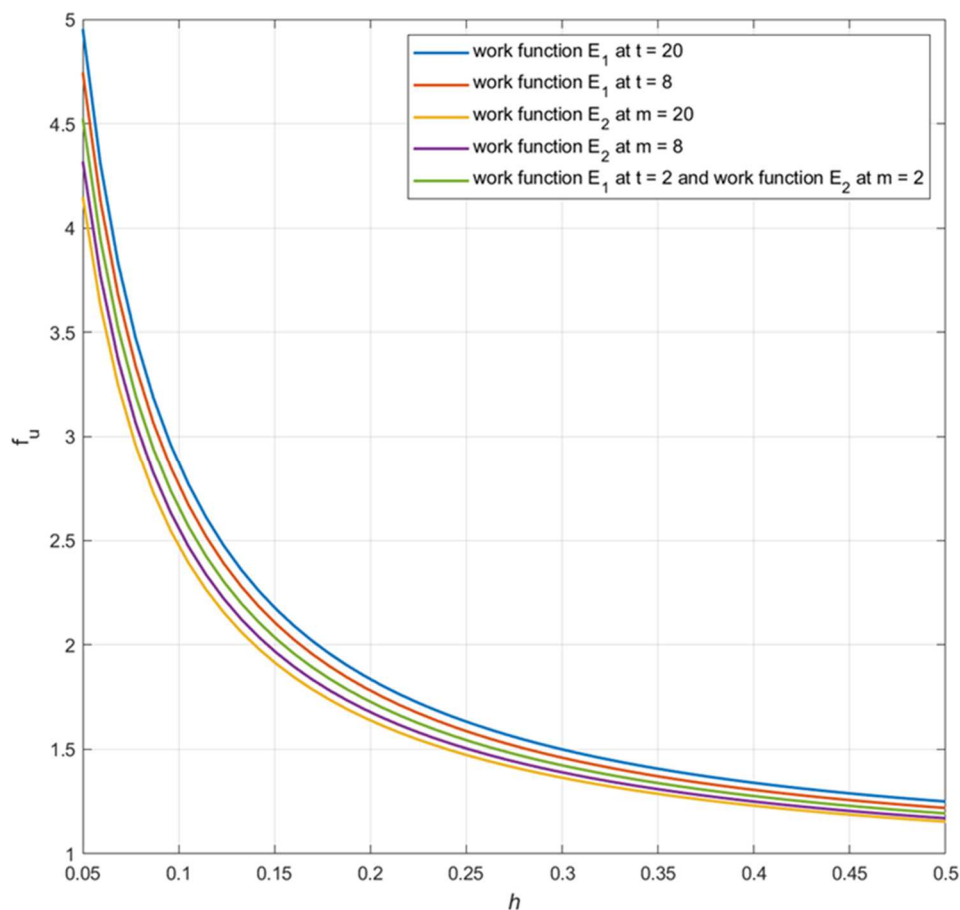
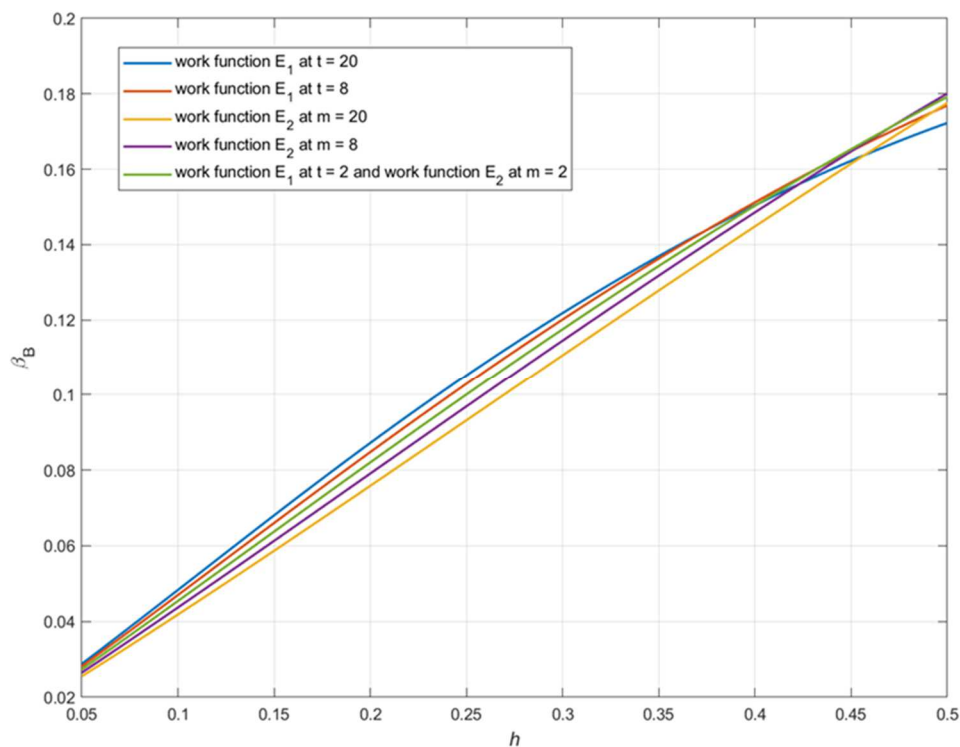


Fig. 3. Verification of the solution.



Fig. 4. Effect of the work function on the limit load at $\alpha = 0.1$.Fig. 5. Illustration that the inequality in (22) is satisfied at $\alpha = 0.1$.

It remains to substitute equations (50) and (51) into equations (34), (41), and (44) and evaluate the integrals numerically. The right-hand side of equation (46) so calculated depends on β_B . Minimizing with respect to this parameter provides the best upper bound based on the kinematically admissible velocity field chosen.



5.2. Verification of the solution

An upper bound solution for the von Mises yield criterion has been presented in [23]. This paper has considered the compression of a solid disk. However, it is immaterial for comparison with the solution for the tensile specimen with no crack since the yield criterion is pressure-independent. Figure 3 depicts the dependence of the dimensionless upper bound limit load on h found in [23] and the new solution for the work functions associated with the von Mises yield criterion (i.e., $t = 2$ in E_1 and $m = 2$ in E_2). The upper bound theorem states that a more accurate solution supplies a lower limit load. It is seen from Figure 3 that the new solution is more accurate than the solution [23]. It is a consequence of a more realistic kinematically admissible velocity field whose behavior near the plane of symmetry and contact surface coincides with that of the real velocity field. Another upper bound solution for the von Mises yield criterion has been presented in [17]. The dependence of the dimensionless upper bound limit load on h found in this work is also shown in Fig. 3. The solution [17] accounts for the behavior of the real velocity field near the plane of symmetry and contact surface. Therefore, it predicts a more accurate limit load than the solution [23]. However, the new limit load solution is more accurate than the solution [17]. It results from a more realistic shape of the velocity discontinuity surface AB in the new solution. The results presented in [17] has also derived a solution for Tresca's yield criterion. The work function E_2 closely approximates Tresca's yield criterion if m is large enough. The calculation has been carried out at $m = 20$. Figure 3 illustrates that the new solution is more accurate than the solution [17].

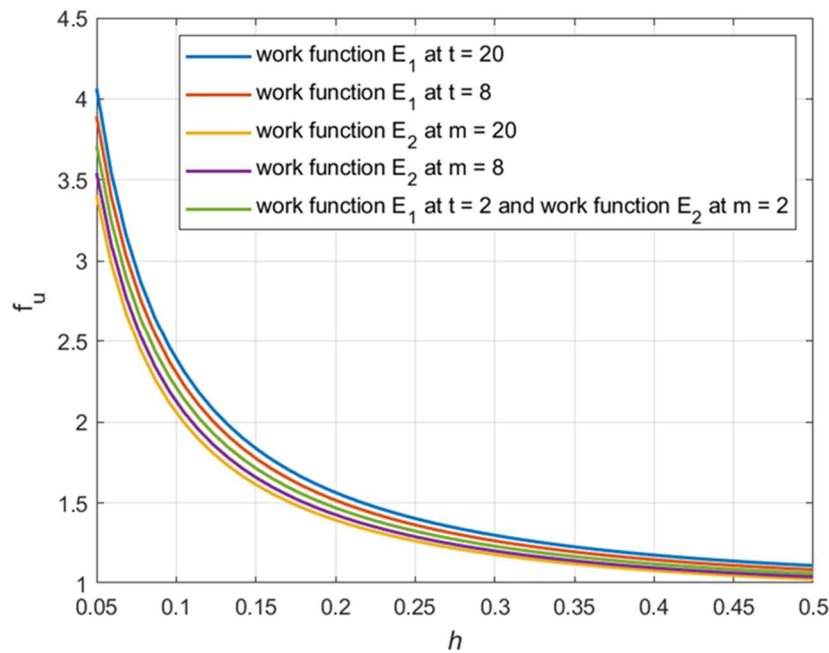


Fig. 6. Effect of the work function on the limit load at $\alpha = 0.3$.

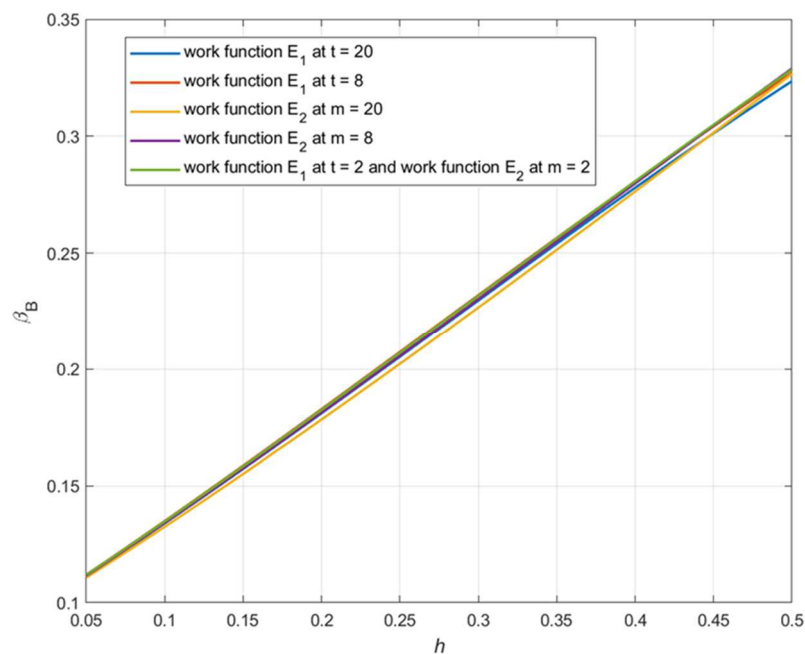


Fig. 7. Illustration that the inequality in (22) is satisfied at $\alpha = 0.3$.



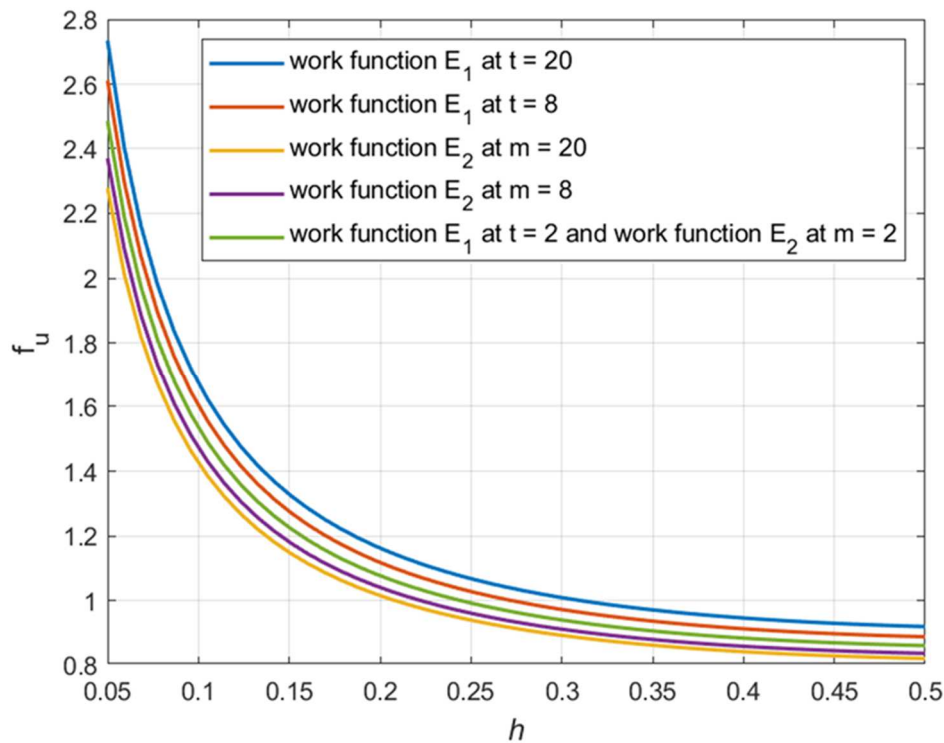


Fig. 8. Effect of the work function on the limit load at $a = 0.5$.

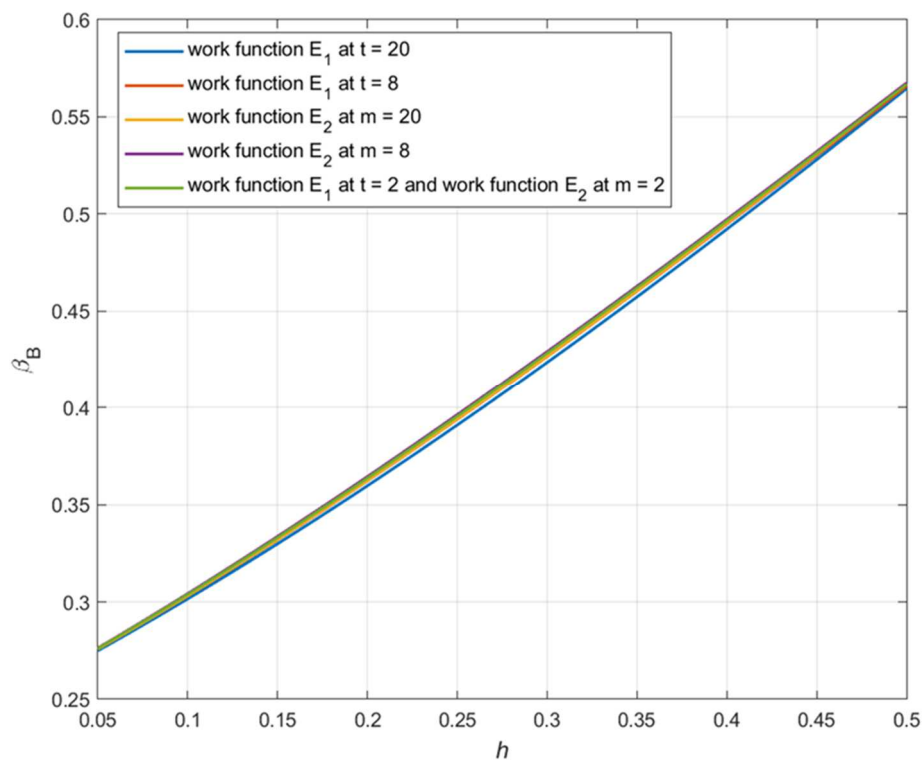


Fig. 9. Illustration that the inequality in (22) is satisfied at $a = 0.5$.

5.3. Effect of the yield criterion on the limit load

The numerical solution is illustrated in Figs. 4 to 9. In particular, Figs. 4, 6, and 8 depict the dependence of the dimensionless limit load on h at $a = 0.1$, $a = 0.3$, and $a = 0.5$, respectively. The different curves in these figures illustrate the effect of the work function or the yield criterion on the limit load. Figures 5, 7, and 9 together with equation (21) show that the inequality in (22) is satisfied. These numerical results are in agreement with physical expectations. In particular, the limit load increases as the yield surface moves from Tresca's hexagon ($m \rightarrow \infty$) to Mises' circle ($m = 2$ and $t = 2$) and then to Schmidt-Ishlinskii's hexagon ($t \rightarrow \infty$). Also, the limit load increases as h decreases independently of other parameters.



6. Conclusion

A new upper bound solution for a round highly undermatched welded bar subject to tension has been derived. The weld contains a circular crack. A distinguished feature of this solution is that it is valid for quite an arbitrary isotropic yield criterion. The version of the upper bound theorem that has never been used in fracture mechanics has been adopted to achieve this result. The solution has been compared to available solutions for the von Mises and Tresca yield criteria found using the standard version of the theorem. It has been shown that the new solution predicts a more accurate limit load. It results from using the singular kinematically admissible velocity field and a realistic shape of one of the velocity discontinuity surfaces. The effect of the work function and geometric parameters on the limit load has been comprehensively illustrated. The solution can be readily applied for evaluating this effect on the prediction of analytical flaw assessment procedures.

Author Contributions

S. Alexandrov: formal analysis and writing—original draft; S. Strashnov: formal analysis and writing—original draft; Y. Li: conceptualization and supervision. The manuscript was written through the contribution of all authors. All authors discussed the results, reviewed, and approved the final version of the manuscript.

Acknowledgments

This paper has been supported by the RUDN University Strategic Academic Leadership Program.

Conflict of Interest

The authors declared no potential conflicts of interest concerning the research, authorship, and publication of this article.

Funding

This research has been supported by the Foreign Expert Project from the Ministry of Science and Technology of China (G2022177004L)

Data Availability Statements


Not applicable.


References

- [1] Schwalbe, K.-H., Kalluri, S., McGaw, R.M., Neimitz, A., Dean, S.W. On the Beauty of Analytical Models for Fatigue Crack Propagation and Fracture—A Personal Historical Review, *Journal of ASTM International*, 7, 2010, 102713, doi:10.1520/JAI102713.
- [2] Zerbst, U., Madia, M., Analytical Flaw Assessment, *Engineering Fracture Mechanics*, 187, 2018, 316–367, doi:10.1016/j.engfracmech.2017.12.002.
- [3] Konjatic, P., Katinic, M., Kozak, D., Gubeljak, N., Yield Load Solutions for SE(B) Fracture Toughness Specimen with I-Shaped Heterogeneous Weld, *Materials*, 15, 2021, 214, doi:10.3390/ma15010214.
- [4] Njock Bayock, F., Kah, P., Mvola, B., Layus, P., Effect of Heat Input and Undermatched Filler Wire on the Microstructure and Mechanical Properties of Dissimilar S700MC/S960QC High-Strength Steels, *Metals*, 9, 2019, 883, doi:10.3390/met9080883.
- [5] Zhao, H., Li, X., Lie, S.T., Strain-Based Fracture Assessment for an Interface Crack in Clad Pipes under Complicated Loading Conditions, *Ocean Engineering*, 198, 2020, 106992, doi:10.1016/j.oceaneng.2020.106992.
- [6] Tümer, M., Warchomicka, F.G., Pahr, H., Enzinger, N., Mechanical and Microstructural Characterization of Solid Wire Undermatched Multilayer Welded S1100MC in Different Positions, *Journal of Manufacturing Processes*, 73, 2022, 849–860, doi:10.1016/j.jmapro.2021.11.021.
- [7] Milošević, N.Z., Sedmak, A.S., Bakic, G.M., Lazic, V., Milošević, M., Mladenovic, G., Maslarevic, A., Determination of the Actual Stress–Strain Diagram for Undermatching Welded Joint Using DIC and FEM, *Materials*, 14, 2021, 4691, doi:10.3390/ma14164691.
- [8] Kim, Y.-J., Schwalbe, K.-H., Compendium of Yield Load Solutions for Strength Mis-Matched DE(T), SE(B) and C(T) Specimens, *Engineering Fracture Mechanics*, 68, 2001, 1137–1151, doi:10.1016/S0013-7944(01)00016-9.
- [9] Hao, S., Cornec, A., Schwalbe, K.H., Plastic stress-strain fields and limit loads of a plane strain cracked tensile panel with a mismatched welded joint, *International Journal of Solids and Structures*, 34(3), 1997, 297–326, doi:10.1016/S0020-7683(96)00021-2.
- [10] Drucker, D.C., Prager, W., Greenberg, H.J., Extended Limit Design Theorems for Continuous Media, *Quarterly of Applied Mathematics*, 9, 1952, 381–389, doi:10.1090/qam/45573.
- [11] Hill, R., *The Mathematical Theory of Plasticity*, Clarendon Press, Oxford, UK, 1950.
- [12] Hill, R., Lee, E.H., Tupper, S.J., A Method of Numerical Analysis of Plastic Flow in Plane Strain and Its Application to the Compression of a Ductile Material Between Rough Plates, *Journal of Applied Mechanics*, 18(1), 1951, 46–52.
- [13] Alexandrov, S., Chung, K.-H., Chung, K., Effect of Plastic Anisotropy of Weld on Limit Load of Undermatched Middle Cracked Tension Specimens, *Fatigue & Fracture of Engineering Materials & Structures*, 30, 2007, 333–341, doi:10.1111/j.1460-2695.2007.01110.x.
- [14] Alexandrov, S., Lyamina, E., Pirumov, A., Nguyen, D.K., A Limit Load Solution for Anisotropic Welded Cracked Plates in Pure Bending, *Symmetry*, 12, 2020, 1764, doi:10.3390/sym12111764.
- [15] Lyamina, E., Kalenova, N., Nguyen, D.K., Influence of Plastic Anisotropy on the Limit Load of an Overmatched Cracked Tension Specimen, *Symmetry*, 12, 2020, 1079, doi:10.3390/sym12071079.
- [16] Arandelovic, M., Sedmak, S., Jovicic, R., Perkovic, S., Burzic, Z., Radu, D., Radakovic, Z., Numerical and Experimental Investigations of Fracture Behaviour of Welded Joints with Multiple Defects, *Materials*, 14, 2021, 4832, doi:10.3390/ma14174832.
- [17] Alexandrov, S.E., Goldstein, R.V., Tchikanova, N.N., Upper Bound Limit Load Solutions for a Round Welded Bar with an Internal Axisymmetric Crack, *Fatigue & Fracture of Engineering Materials & Structures*, 22, 1999, 775–780, doi:10.1046/j.1460-2695.1999.t01-1-00208.x.
- [18] Hill, R., New Horizons in the Mechanics of Solids, *Journal of the Mechanics and Physics of Solids*, 5, 1956, 66–74, doi:10.1016/0022-5096(56)90009-6.
- [19] Alexandrov, S., Lyamina, E., Jeng, Y.-R., Application of the Upper Bound Theorem for Metal Forming Processes Considering an Arbitrary Isotropic Pressure-Independent Yield Criterion with No Strength Differential Effect, *International Journal of Advanced Manufacturing Technology*, 126, 2023, 3311–3321, doi:10.1007/s00170-023-11312-5.
- [20] Hosford, W.F., A Generalized Isotropic Yield Criterion, *Journal of Applied Mechanics*, 39, 1972, 607–609, doi:10.1115/1.3422732.
- [21] Alexandrov, S., Richmond, O., Singular Plastic Flow Fields near Surfaces of Maximum Friction Stress, *International Journal of Non-Linear Mechanics*, 36, 2001, 1–11, doi:10.1016/S0020-7462(99)00075-X.
- [22] Alexandrov, S., Richmond, O., On Estimating the Tensile Strength of an Adhesive Plastic Layer of Arbitrary Simply Connected Contour, *International Journal of Solids and Structures*, 37, 2000, 669–686, doi:10.1016/S0020-7683(99)00023-2.
- [23] Kudo, H., Some Analytical and Experimental Studies of Axi-Symmetric Cold Forging and Extrusion—I, *International Journal of Mechanical Sciences*, 2, 1960, 102–127, doi:10.1016/0020-7403(60)90016-3.



ORCID iD

Sergei Alexandrov  <https://orcid.org/0000-0001-7289-0856>

Stanislav Strashnov  <https://orcid.org/0000-0002-6401-2524>

Yong Li  <https://orcid.org/0000-0002-8008-0375>



© 2024 Shahid Chamran University of Ahvaz, Ahvaz, Iran. This article is an open access article distributed under the terms and conditions of the Creative Commons Attribution-NonCommercial 4.0 International (CC BY-NC 4.0 license) (<http://creativecommons.org/licenses/by-nc/4.0/>).

How to cite this article: Alexandrov S., Strashnov S., Li Y. Application of a Generalized Isotropic Yield Criterion to Determining Limit Load Solutions for Highly Undermatched Welded Bars in Tension, *J. Appl. Comput. Mech.*, 10(3), 2024, 443–454. <https://doi.org/10.22055/jacm.2024.44923.4289>

Publisher's Note Shahid Chamran University of Ahvaz remains neutral with regard to jurisdictional claims in published maps and institutional affiliations.

